

## THE POTENTIAL AMELIORATIVE EFFECT OF WHEY PROTEIN ON CIRCUMVALLATE PAPILLA AND ASSOCIATED STRUCTURES OF STREPTOZOTOCIN-INDUCED DIABETIC RATS

Fatema A. Al-Sayed <sup>\*ID</sup>, Mai Abdelhalim Hamouda <sup>\*\*ID</sup> and Sana Mostafa <sup>ID</sup>

### ABSTRACT

**Background:** Diabetes mellitus-induced oxidative stress is considered a major problem that causes several adverse consequences. Among the commonly known natural antioxidants is whey protein (WP), as it reduces oxidative stress and supports immune system performance..

**Aim:** The present study aimed to assess the influence of WP in ameliorating the destructive effect of induced type 1 Diabetes Mellitus (T1DM) on the circumvallate papilla (CVP) structure in rats' tongue.

**Methodology:** Eighteen rats were distributed into three groups; group I served as control, and T1DM was induced in the other 2 groups by individual injection of streptozotocin (60 mg/kg body weight) intraperitoneally. After confirmation of diabetes induction, rats were distributed in group II (received no treatment) and group III (received WP at a dose of 0.3 gm/kg for four weeks). The CVPs were examined for histopathological, histomorphometric analysis of taste buds' count, and immunohistochemical analysis of Nrf2 protein.

**Results:** Histological and histomorphometric results exhibited apparent tissue degeneration in group II including taste buds, CVP ganglion, von Ebner's gland, and muscles. Group III revealed marked improvement in all tissue components with an image closer to control. Immunohistochemical analysis of Nrf2 protein revealed the highest expression in group II while administering WP suppressed Nrf2 expression in group III.

**Conclusion:** Oral administration of WP showed a remarkable ability to counteract the damage induced by T1DM in CVP tissues and reduced oxidative stress levels.

**KEYWORDS:** Diabetes Milletus, Whey Protein, Circumvallate papilla ganglion, von Ebner's Salivary Gland, Nrf2

\* Lecturer, Oral Biology Department, Faculty of Dentistry, Cairo University, Cairo, Egypt.

\*\* Lecturer of Oral pathology, Faculty of Dentistry, King Salman International University, El-Tur.

## INTRODUCTION

Diabetes Mellitus (DM) is a chronic metabolic disease that has affected many people in the world.<sup>(1)</sup> Universally, about 537 million adults have been diagnosed by DM in 2021 and the prevalence is expected to witness an increase of 46% by 2045.<sup>(2)</sup> DM is manifested as two common forms; Type 1 (T1DM) that results from autoimmune  $\beta$ -cell destruction and type 2 (T2DM) that caused by continuing loss of  $\beta$ -cell insulin secretion, with hyperglycemia as a shared outcome in both types.<sup>(3)</sup>

The majority of the reported fatal cases have principally resulted from micro and macrovascular complications that arise secondary to the persistent hyperglycemia during the onset of the disease.<sup>(1)</sup> DM is linked to different oral complications, involving xerostomia, gingivitis, periodontitis, and increased vulnerability to oral infections.<sup>(4)</sup> Several studies have reported the effect of DM in taste impairment, including altered taste and morphological changes in fungiform and circumvallate papillae (CVP).<sup>(5)</sup>

Oxidative stress and inflammation are considered fundamental factors in DM progression.<sup>(1)</sup> Hyperglycemia and free fatty acids leads to excessive formation of reactive oxygen species (ROS) and defective antioxidants defensive mechanism.<sup>(6)</sup> The ROS trigger several intracellular signaling pathways that finally initiates insulin resistance, damaged  $\beta$ -cell of the pancreas, defected glucose tolerance and malfunction of the mitochondria.<sup>(4,6)</sup> Mitochondria is the main origin of oxidative stress in DM which eventually leads to the accumulation of chronic oxidative stress in many organs.<sup>(7,8)</sup>

Whey protein (WP) is a yellow-green-colored liquid derived from milk that is obtained after separation of the curd during milk coagulation using proteolytic enzymes or acids. Recently, it has been recognized as a functional source of nutrients that having several health benefits.<sup>(9)</sup> It is a well-known derivation of glutamine and the branched-chain amino acids (BCAAs), that are necessary for cell growth. Several BCAAs like leucine, isoleucine

and valine were documented to enhance the bones, skin and muscle tissues healing. Moreover, Leucine stimulates glutamate dehydrogenase activity that raises the Krebs cycle's activity and the cells' consumption of oxygen, which in turn elevates the synthesis of insulin.<sup>(10,11)</sup>

WP has been reported to promote secretion of insulin and decrease glycemic levels in diabetic patients.<sup>(9)</sup> Multiple studies revealed the ability of WP protein in ameliorating inflammation and reducing oxidative stress. WP protein can activate the endogenous antioxidative system and control lipid peroxidation, free radicals and ROS levels. It enhances the production of reduced glutathione (GSH) and enhances the synthesis of pro- and post-inflammatory cytokines.<sup>(10,11)</sup>

One important transcription factor that controls a wide range of detoxifying and antioxidant enzymes is nuclear factor erythroid-2-related factor-2 (Nrf2). Its activation helps in the protection of cells from oxidative damage. Therefore, Nrf2 is crucial in preventing complications from hyperglycemia in DM, as its deficiency contribute to elevation of ROS level, leading to hyperglycemia and impaired insulin signaling.<sup>(6,7,12)</sup>

Circumvallate papilla (CVP) is a distinctive gustatory apparatus, that has a fundamental role in taste perception. Within the core of the papilla, an intrinsic ganglion called the CVP ganglion were located. It plays a primary function in taste perception and taste cells modulation<sup>(13)</sup>. Streptozotocin (STZ) drug can employ selective damage to pancreatic  $\beta$ -cells which affect insulin secretion and cause hyperglycemia. Thus, it has been widely used to examine the complications of DM in animals' models<sup>(14)</sup>. Consequently, the current work objective is to explore the influence of WP in ameliorating the effect of STZ-induced T1DM on the CVP structure in rats by means of histological, immunohistochemical and Histomorphometric analyses.

## MATERIALS AND METHODS

### Materials

STZ in the form of powder was purchased from Sigma, Egypt. WP concentrate-80 solution (WPC-80) in the form of powder was purchased from Pharma First, Egypt.

### Ethical approval

The present study was permitted by the Institutional Animal Care and Use Committee (IACUC) - Cairo University (Approval code: CU-III-F-C/32/24). The ARRIVE principles and procedures were followed for conducting this study (<https://arriveguidelines.org>).

### Sample size calculation

As per previous study; **Yasser & Shon**, we calculated that the minimum proper sample size was 6 rats in each arm with a total sample of 18 rats to be able to reject the null hypothesis with 95% power at  $\alpha = 0.05$  level using Student's t test for independent samples. Sample size calculation was done using Stats Direct statistical software version 2.7.2 for MS Windows, StatsDirect Ltd., Cheshire, UK. <sup>(15)</sup>

### Animals

Eighteen healthy adults male Wistar rats (180-220 grams) were acquired from animal house of Faculty of Medicine, Cairo University. Rats were kept under controlled room temperature of  $22\pm 3^{\circ}\text{C}$  and humidity of 50–60% with 12:12h light/dark cycles in polycarbonate cages and allowed free

access to food and water. The attending veterinarian was responsible for evaluating the animals' welfare in accordance with the moral guidelines for treating animals.

### Study design

Study design is described in **table 1**. The rats were randomly distributed after one week acclimatization period into three groups (6 rats each) as follows:

**Group I (Control group):** normal rats received only saline intraperitoneally (IP). **Group II:** DM were induced by a single IP injection of STZ at a dose of 60 mg/kg body weight, without receiving treatment till end of experiment. <sup>(16)</sup> **Group III:** DM were induced as previous group and followed by daily administration of WPC-80 at a dose of 0.3 gm/kg starting one week following induction of DM for 4 weeks. <sup>(17)</sup> Doses of WPC-80 were administered by oral gavage using a needle fitted to a disposable syringe. Rats from all groups were euthanized after 5 weeks from the start of experiment with excessive dosage of sodium thiopental (80mg/kg; IV) (Sigma Tec Pharma – Egypt) <sup>(18)</sup> and death was confirmed by head decapitation.

### Induction of DM

Twelve rats were assigned for DM induction. Before the beginning, one blood drop was taken from the tail vein of each animal. The blood glucose level was determined using a Fine test™ Auto Coding Premium blood glucose meter (Osang Healthcare Co., Ltd, South Korea). Rats typically have blood glucose levels between 80 and 120 mg/dl.

TABLE (1) Summary of the study design

Group	Status	Intervention	Time of intervention	Route of injection
Group I	Non-diabetic (Control)	Saline	At start of experiment	IP
Group II	Diabetic	STZ	At start of experiment	IP
Group III	Diabetic	STZ WP	At start of experiment After one week	IP Oral

DM was induced in groups 2 and 3 by single IP injection of STZ at dose of 60 mg/kg (Sigma, St. Louis, MO, USA) that was dissolved in freshly prepared 0.01 M citrate buffer (pH 4.5) and injected in the overnight fasted rats to induce T1DM. Three days after the induction of DM, blood samples were obtained from the rats to measure the blood glucose. Rats with blood glucose less than 200 mg/dl were excluded from the experiment. The remaining included rats were randomly distributed among the two experimental groups. The blood glucose level was measured once per week till the day of euthanasia. All animals were examined for any behavioral changes and abnormal clinical signs daily. Weights and blood glucose levels were measured before euthanasia.

### **Histopathological examination**

CVPs were dissected from the base of the tongue of all rats and directly fixed in 10% neutral formalin for 24 hours, then washed to remove excess fixative. The samples were dehydrated in ascending grades of ethanol, cleared in xylene, and embedded in paraffin wax according to standard protocol<sup>(19)</sup>. Sections of 4-5  $\mu\text{m}$  were cut using a microtome (LEICA RM2255, Leica Biosystems, Nussloch GmbH). The sections fixed to normal slides for hematoxylin and eosin (H&E) staining (Sigma®, St. Louis, MO, USA) and to charged slides for immunohistochemical (IHC) staining to ensure sections adherence. The slides were examined using a Leica RM2255 light microscope (Leica Microsystems, Inc., Switzerland) equipped with digital camera and image analysis software.

### **Immunohistochemical localization of Nrf2 protein**

Tissue sections were deparaffinized, hydrated, and subsequently subjected to antigen retrieval by boiling in mixture of 10 mM Tris/1 mM EDTA (pH 9) for 18 minutes, then cooled to room temperature. To quench the endogenous peroxidase activity, tissue sections were incubated in 3% hydrogen peroxide for

10 minutes, then blocked with 100–400  $\mu\text{l}$  blocking solution for 1 hour to prevent non-specific binding of the antibody. The blocking solution was removed and 100–400  $\mu\text{l}$  of diluted primary antibody for Nrf2 Polyclonal Antibody (Product # PA1-38312) (Invitrogen, ThermoScientific, USA), was added at dilution of 1:250 and incubated at 4°C overnight in a humidified chamber. The sections washed in wash buffer, then incubated with 1–3 drops EnVision FLEX link Detection Reagent, cat no: K8000 (Dako, Denmark) in a humidified chamber for 30 minutes. A mixture of 30  $\mu\text{l}$  of DAB Chromogen Concentrate and 1 ml of DAB Diluent were used, then a 100–400  $\mu\text{l}$  SignalStain® DAB was applied to each section and monitored closely for 1–10 until provides an acceptable staining intensity, followed by counter staining with hematoxylin for better visualization of tissue morphology. The evaluation of immuno-staining was performed by expert blinded pathologist and H -score was calculated according to **Ram et al., 2021.**<sup>(20)</sup>

### **Histomorphometric analysis:**

Each papilla's taste buds count was calculated in accordance with Pai et al. (2007). Twenty taste buds were marked at random in each sample, and the number of sections required for each one to fully appear was recorded. The total taste buds count was then determined by dividing this average by the total number of sections.<sup>(21)</sup> After labeling each slice with green crosses, the taste buds were calculated using the Image J (Version:1.53t) image analysis software. Each segment was viewed at a magnification of x100. One calibrated, blinded examiner performed all the measurements.

The area percentage (%) of the detected color of the positive immunohistochemically stained cells were performed using the Image J software. Six fields were selected randomly for each section at x100 magnification, and the mean values were calculated from each sample.

### Statistical analysis

Data were analyzed using the statistical package SPSS version 22. Data were described in terms of mean and standard deviation. Data were checked for normality; data were normally distributed and were analyzed using ANOVA test followed by multiple comparison Tukey post hoc test.

## RESULTS

### Histopathological results

The histopathological examination of **group I** displayed normal CVP outline, the gustatory epithelium contained many mature taste buds with taste pore opening into a deep trough (**Figs.1-a, 1-d**). CVP ganglion was located at the connective tissue core enclosing multiple large, rounded ganglion cells with eccentric nuclei (**Fig.1-d**). The connective tissue include normal shaped von Ebner's glands (VEGs) tissue dispersed among normally aligned intrinsic muscle bundles (**Figs.1-a, 2-a**).

**Group II** revealed marked outline deformity as the papilla was smaller in size and bounded by short troughs. The gustatory epithelium comprised a few enlarged taste buds with signs of degeneration and taste cells' separation (**Figs.1-b, 1-e**). The ganglion tissue was degenerated and invaded by marked inflammatory cells infiltrate and congested blood vessels (**Fig.1-e**). VEGs' serous acini appeared degenerated, shrunken and atrophied with pyknotic nuclei and extensive cytoplasmic vacuolization. All muscles groups displayed marked degeneration and separation between bundles (**Figs.1-b, 2-b**).

**Group III** exhibited a normal papilla outline and surrounded by deep troughs. The gustatory epithelium comprised multiple mature taste buds (**Figs.1-c, 1-f**). The ganglion tissue contained normal shaped ganglion cells and was surrounded by moderate inflammatory cells (**Fig.1-f**). Normally shaped VEGs acini with few cytoplasmic vacuolization and increased spaces between lobules

was observed. Muscle bundles were normally aligned while some of them showed signs of degeneration and separation between muscle fibers (**Fig.1-c, 2-c**).

### Immunohistochemical results

Immunohistochemical expression of Nrf2 of **group I** revealed negative to weak immunoreactivity in serous acini of VEGs and surrounded muscles, and strong positive cytoplasmic staining in some myoepithelial cells (**Fig.2-d**). **Group II** displayed moderate to strong nuclear immunoreactivity in both serous acini of VEGs and myoepithelial cells, whereas muscles exhibited moderate staining (**Fig.2-e**). **Group III** showed weak to moderate immunoreactivity in both serous acini of VEGs and myoepithelial cells, but muscles exhibited negative staining (**Fig.2-f**).

### Statistical results

#### *Nfr2 area percentage*

The highest mean area percentage was recorded in group II, while the lowest value was recorded in group I (control group) with statistically significant difference between groups ( $p < 0.05$ ) (**Table 2**). Pair wise comparison revealed a statistically significant higher Nfr2 area percentage in group II as compared to both group I and group III ( $p < 0.05$ ). While the difference between group III and group I was not statistically significant (**Table 3**).

#### *Number of taste buds*

The highest mean number of taste buds was recorded in group I while the lowest value was recorded in group II with a statistically significant difference between groups ( $p < 0.05$ ) (**Table 4**). Pair wise comparison revealed a statistically significant higher number of taste buds in group I as compared to both group II and group III ( $p < 0.05$ ). Also, a statistically significant higher number of taste buds was observed in group III as compared to group II ( $p = 0.01$ ) (**Table 5**).

TABLE (2) Descriptive statistics and comparison between groups for Nfr2 area percent (ANOVA test)

	Group	Mean $\pm$ SD	Std. Error	Min	Max	95% Confidence Interval for Mean	P value
Nfr2 area percent	Group III	3.817 $\pm$ 0.697 <sup>B</sup>	0.285	2.600	4.500	(3.193, 4.441)	0.000*
	Group II	5.950 $\pm$ 0.946 <sup>A</sup>	0.386	4.700	7.100	(5.326, 6.574)	
	Group I	2.867 $\pm$ 0.403 <sup>B</sup>	0.165	2.300	3.300	(2.243, 3.491)	

*Significance level  $P < 0.05$ , \*significant, means with different superscript letters are significantly different*

TABLE (3) Detailed results of Tukey's post hoc test for pairwise comparison of area percent.

	Difference of Levels		95% Confidence Interval	P-Value
Nfr2 area percent	Group II	Group III	(1.059, 3.208)	0.000*
	Group I	Group III	(-2.025, 0.125)	0.088
		Group II	(-4.158, -2.009)	0.000*

*Significance level  $P < 0.05$ , \*significant.*

TABLE (4) Descriptive statistics and comparison between groups for Number of taste buds (ANOVA test)

Number of taste buds	Mean $\pm$ SD	Std. Error	Min	Max	95% Confidence Interval for Mean	P value
Group I	324.7 $\pm$ 37.7 <sup>A</sup>	15.4	280.0	375.0	(301.0, 348.3)	0.000*
Group II	97.33 $\pm$ 8.59 <sup>C</sup>	3.51	87.00	112.00	(73.65, 121.01)	
Group III	172.7 $\pm$ 26.9 <sup>B</sup>	11.0	130.0	202.0	(149.0, 196.3)	

*Significance level  $P < 0.05$ , \*significant, means with different superscript letters are significantly different*

TABLE (5) Detailed results of Tukey's post hoc test for Number of taste buds

Difference of Levels		95% Confidence Interval	P-Value
Group II	Group I	(-268.1, -186.6)	0.000*
Group III	Group I	(-192.8, -111.2)	0.000*
	Group II	(34.6, 116.1)	0.001*

*Significance level  $P \leq 0.05$ , \*significant*

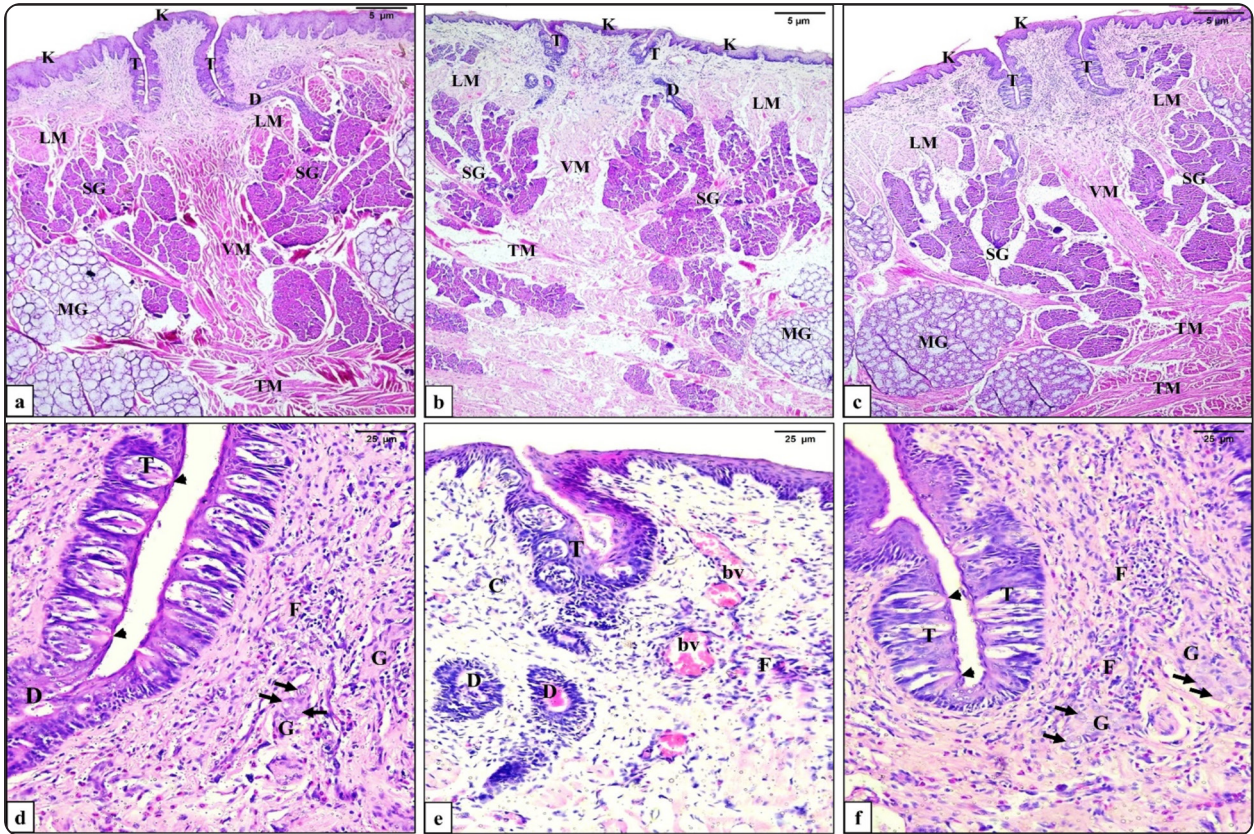


**Fig. (1)** Photomicrographs of rats' CVP showing; **a) Group I:** normal shaped CVP papilla outline bounded by deep troughs, with normal keratinized epithelium (K), the gustatory epithelium comprised multiple taste buds (T), and the underlying connective tissue include normal shaped von Ebner's gland (SG) dispersed among normally aligned muscle bundles including longitudinal group (LM), vertical group (VM) and Transverse group (TM). **b) Group II:** Marked outline deformity of the papilla with thin covering epithelium (K) that surrounded by short troughs, the gustatory epithelium comprise few swollen, degenerated taste buds (T), the von Ebner's glands' acini appeared shrunken with wide spaces in-between (SG), and all muscles groups displayed marked degeneration and separation between bundles (LM, VM, TM). **c) Group III:** normal papilla outline and surrounded by deep troughs, with covering epithelium of moderate thickness (K), the gustatory epithelium comprised multiple taste buds (T), normal shaped von Ebner's gland with increased spaces between lobules (SG), and normally aligned muscle bundles of all groups (LM, VM, TM) (H&E, Orig. Mag. X40). **d)** Higher magnification of **group I** displaying normal mature taste buds (T) with taste pores (arrow heads), normal ganglion tissue (G) enclosing normal shaped rounded ganglion cells (short arrows), with few inflammatory cells (F). **e)** Higher magnification of **group II** showing few swollen degenerated immature taste buds (T), degenerated ganglion tissue that was invaded by marked inflammatory cells infiltrate (F) and congested blood vessels (bv), with degeneration and disorientation of collagen fibers (C). **f)** Higher magnification of **group III** presenting normal shaped taste buds (T) with taste pore (arrowheads), normal ganglion tissue (G) with normal shaped ganglion cells (arrows) and infiltrated by moderate inflammatory cells (F) (H&E, Orig. Mag. X200). MG: Mucous gland, D: Duct.

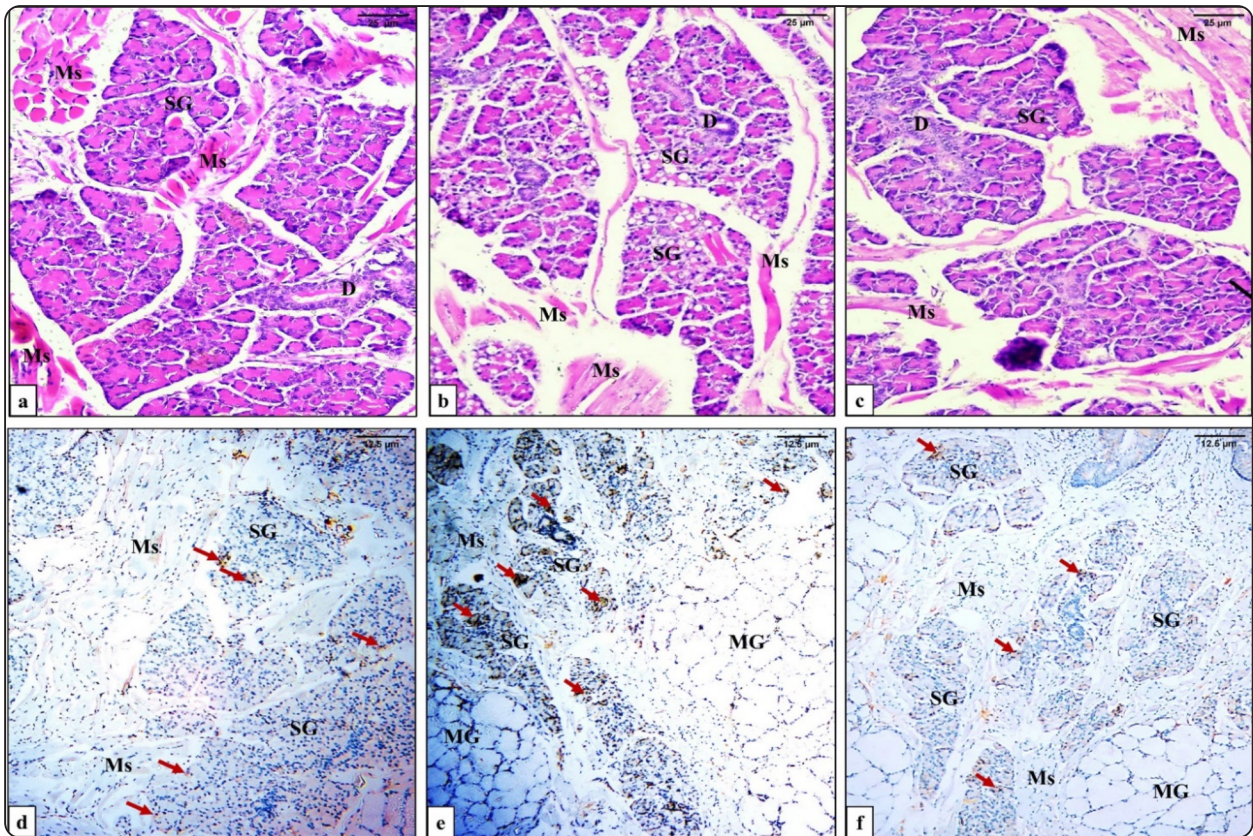


**Fig. (2):** Photomicrographs of rats' CVP showing: **a) Group I:** normal serous acini of VEGs with basophilic cytoplasm (SG), normal epithelial lining of the duct (D), and normal aligned muscle fibers around and between gland lobes (Ms) **b) Group II:** increased spacing between degenerated and atrophied serous acini with pyknotic nuclei and extensive cytoplasmic vacuolization (SG), the duct lining showed darkly stained nuclei (D), degenerated muscle fibers with separation between muscle fibers (Ms) **c) Group III:** normal shaped serous acini with few cytoplasmic vacuolization (SG), indefinite duct outline with open faced nuclei (D), some muscle fibers showed signs of degeneration and separation between muscle fibers (Ms) (H&E, Orig. Mag. X200). Photomicrographs of Immunohistochemical expression of Nrf2 showing **d) Group I:** negative or weak immunoreactivity was observed in serous acini of VEGs (SG) and muscles (Ms), and strong positive cytoplasmic staining in some myoepithelial cells (red arrows). **e) Group II:** displayed moderate to strong nuclear immunoreactivity in both serous acini of VEGs (SG) and myoepithelial cells (red arrows), while muscles displayed moderate staining (Ms). **f) Group III:** showed weak to moderate immunoreactivity in both serous acini of VEGs (SG) and myoepithelial cells (red arrows), muscles exhibited negative staining (Ms) (Nrf2 immunostain, Orig. Mag. X100). MG: Mucous gland.

## DISCUSSION

It is well known that inadequate levels of the antioxidant defense mechanism in diabetic patients make them susceptible to oxidative stress.<sup>(22)</sup> Hence, there is a critical need to investigate antioxidative reagents for overcoming various stressful stimuli. WP has been demonstrated in previous research to alleviate oxidative stress

in endothelial cells, muscles, malignancies, and DM.<sup>(23,24,25,26)</sup> In the present study, the histopathological results showed that in comparison to control group, the diabetic untreated group (group II) presented apparent degeneration of the papilla structure manifested by fewer taste buds' number with signs of degeneration, degenerated ganglion tissue that was invaded by inflammatory cells, atrophied and degenerated VEGs' acini with pyknotic nuclei



as well as extensive cytoplasmic vacuolization, and all muscles groups displayed marked degeneration and separation between its fibers.

In accordance with this finding, it was proven that STZ-induced DM in rats causes degeneration and reduces the number of both taste buds and ganglion cells in CVP. Moreover, DM induced aggregation of inflammatory cells around the ganglion tissue at an onset of 4 weeks in rats. <sup>(21,27)</sup> Furthermore, DM was reported to affect serous acinar cells of submandibular salivary gland and caused evident vacuolization that was pronounced in short-term disease onset (30 days). <sup>(28)</sup> In addition, the skeletal muscles of diabetic rats demonstrated disruption and discontinuity with reduction in thickness of muscle fibers. <sup>(29)</sup> The structural damage that occurred in DM group is probably linked to the elevation of pro-inflammatory cytokines production which provoke oxidative nitrosative stress and inflammation. The inflammatory cytokines subsequently can activate apoptosis, abnormal turnover, and degeneration. <sup>(27)</sup>

Results of group III (diabetic treated with WPC-80) revealed obvious improvement of the histological structure in comparison to group II. The general outline of the papilla was close to normal, and the gustatory epithelium comprised multiple mature taste buds. The CVP ganglion tissue included numerous normal shaped ganglion cells that was surrounded by moderate inflammatory cells infiltration. The VEGs acini histology was closer to normal and showed few cytoplasmic vacuolization. Intrinsic muscles of all groups were normally aligned while some of them showed signs of degeneration between muscle fibers.

Numerous previous studies have proved the beneficial effect of WP in restoring structure and function of different organs of diabetic animals, beside to its anti-hyperglycemic and insulinotropic effect. It was confirmed that oral administration of WP can restore the inflammatory cytokines levels to normal and shorten the time needed for wound healing in induced DM in mice.

Moreover, the antioxidative activity of WP was manifested by significant reduction of the levels of malondialdehyde, ROS, and elevation of the glutathione level. <sup>(11)</sup>

It was found that T1DM treatment by WP recovered the structure of lymphoid tissues and downregulated apoptosis by reducing the proapoptotic Bax and activating the anti-apoptotic Bcl-XL levels in the bone marrow of mice. <sup>(30)</sup> Additionally, it was proved that WP restored the histological structure of spleen, decreased oxidative stress and Fas mRNA expression in the diabetic rats. <sup>(31)</sup>

The WP positive effect on VEGs structure agreed with previous work which concluded that oral administration of WP improved redox status and reduced the oxidative stress index in parotid glands of old rats. <sup>(32)</sup> The current results revealed apparent regeneration and restoring normal orientation of intrinsic muscles of the tongue. WP was documented to increase the level of muscle insulin receptor tyrosine kinase (IRTK) in skeletal muscles. <sup>(10)</sup>

Nrf2 serves as a principal transcription factor regulating the production of numerous cytoprotective enzymes, acting as a master regulator of redox homeostasis. Nrf2 either stays silent or maintains the lowest basal level of activity under normal circumstances. <sup>(33)</sup> This was confirmed by the immunohistochemical results of control group of the present study, which revealed negative to weak immunoreactivity in serous acini of VEGs and surrounded muscles. However, strong positive cytoplasmic staining was detected in some myoepithelial cells. In parallel to our results, **Drożdżik et al.**, revealed that Nrf2 proteins were expressed in myoepithelial cells, whereas acinar cells showed negative expression. <sup>(34)</sup>

Nrf2 is considered as an adaptation mechanism that is induced in cells with elevated blood glucose levels or in diabetic animals and people. <sup>(35)</sup> In the herein study, the highest detection of Nrf2 expression was detected in the diabetic group. This is attributed to the fact that it is well-established that oxidative stress elevates Nrf2 function and expression in both

*in-vitro* cells and *in-vivo* tissues. Consequently, Nrf2's augmented ameliorating effect on diabetes-induced oxidative damage and its accompanying consequences may be explained by the elevation of its expression and function through an array of strategies. <sup>(35,36)</sup>

It has also been suggested that, in the case of acute hyperglycemia, there are increased levels of Nrf2. The elevated Nrf2 levels is predictable considering Nrf2 operates as the body's antioxidant mechanism in stressful situations. <sup>(37)</sup> Nuclear expression rather than cytoplasmic expression of Nrf2 was increased in the diabetic group of the current study. This could be explained by **Dinkova-Kostova & Abramov**, who stated that under normal circumstances, Nrf2 is linked to its negative regulator, Kelch-like ECH-associated protein-1 (Keap1). However, in stressful conditions, this complex breaks up, and Nrf2 moves to the nucleus, where it binds to antioxidant responsive elements and supports several processes, including cellular redox homeostasis and antioxidant activity. <sup>(38)</sup> In agreement with our results a study performed by **To et al.**, reported that non-tumorous liver specimen with minimal oxidative stress revealed cytosolic expression of Nrf2, while in tumorous areas with more severe hepatic inflammation and oxidative stress this cytosolic expression was shifted to dense nuclear Nrf2 staining areas due to nuclear translocation of Nrf2. <sup>(39)</sup>

The immunohistochemical results of group III showed marked decline in Nrf2 expression in comparison to group II. Similarly, **Cheng et al.**, reported that adding WP to human breast cancer cells that shows high glutathione (GSH) and ROS levels, resulted in reduced Nrf2 nuclear accumulation and depleted GSH levels. <sup>(40)</sup> Moreover, **Cheng et al.** discovered that WP supplementation had a potent antioxidative effect in rats with cancers of the mammary glands, reducing the nuclear buildup of Nrf2 in tumor tissue. <sup>(41)</sup> Our results were in line with those of **Kerasiotti et al.**, who previously revealed that WP exhibited antioxidant activity in

endothelial cells via a Nrf2-dependent mechanism. <sup>(24)</sup> The intrinsic muscles of the tongue of the control and treated group showed weak reactivity to Nrf2 staining. According to **Kerasiotti et al.**, the anti-oxidative impact of WP is cell-dependent, which may help to explain our findings. They demonstrated that supplying WP to muscle C2C12 cells had no influence on the expression of Nrf2 in the cells' cytoplasm or nucleus. <sup>(24)</sup>

## CONCLUSIONS

Consequently, it could be concluded that WP offers a potent therapeutic and anti-oxidative effect against the degenerative effect of T1DM in CVP and associated structures in rats. It could be considered that our work demonstrated for the first time how WP counteract STZ-induced DM by controlling the Nrf2 signaling molecule and suggested a possible role for creating functional foods based on WP that promote health advantages.

It was observed that the tongue of diabetic rats treated by WP didn't restore the normal histological architecture nor the Nrf2 expression to the normal control conditions. The short-term experiment duration of four weeks may not reflect the full potential of therapeutic effect of WP against DM complications. Therefore, longer durations of treatment is recommended to be investigated to observe if more improved histological and immunohistochemical effects could be achieved. Additionally, further research is needed to delve deeper into the precise molecular control mechanism of WP against DM.

## REFERENCES

1. Sireesh D, Dhamodharan U, Ezhilarasi K, Vijay V, Ramkumar KM. (2018) Association of NF-E2 related factor 2 (Nrf2) and inflammatory cytokines in recent onset type 2 diabetes mellitus. *Scientific Reports*. 8(1):5126.
2. IDF-International Diabetes Federation; <https://idf.org/about-diabetes/diabetes-facts-figures/>
3. Lin R, Brown F, James S, Jones J, Ekinici E. (2021) Continuous glucose monitoring: a review of the evidence in

- type 1 and 2 diabetes mellitus. *Diabetic Medicine*. 38(5): e14528.
4. Rohani B. (2019) Oral manifestations in patients with diabetes mellitus. *World journal of diabetes*.;10(9):485-9.
  5. Gaida D, Park Y-W, Kim S-G. (2023) 4-Hexylresorcinol and Its Effects on Circumvallate Papillae Taste Buds in Diabetic and Healthy Rats: An Initial Investigation.;13(21):11617.
  6. Tan SM, de Haan JB. (2014) Combating oxidative stress in diabetic complications with Nrf2 activators: how much is too much?. *Redox Report*. 1;19(3):107-17.
  7. Li X, Sun X, Zhang X, Mao Y, Ji Y, Shi L, Cai W, Wang P, Wu G, Gan X, Huang S. (2018) Enhanced oxidative damage and Nrf2 downregulation contribute to the aggravation of periodontitis by diabetes mellitus. *Oxidative Medicine and Cellular Longevity*. (1):9421019.
  8. Behl T, Kaur I, Sehgal A, Sharma E, Kumar A, Grover M, Bungau S. (2021) Unfolding Nrf2 in diabetes mellitus. *Molecular Biology Reports*. 48:927-39.
  9. Lesgards JF. (2023) Benefits of whey proteins on type 2 diabetes mellitus parameters and prevention of cardiovascular diseases. *Nutrients*. 6;15(5):1294.
  10. El-Ashmawy N, Khedr E, El-bahrawy H, El-Mokadem E, Abo-Saif M. (2019) Whey protein upregulates muscle insulin receptor tyrosine kinase and is comparable to vildagliptin as insulin-sensitizer. *Romanian Journal of Diabetes, Nutrition and Metabolic Diseases*. 15;26(4):131-7.
  11. Ebaid H, Salem A, Sayed A, Metwalli A. (2011) Whey protein enhances normal inflammatory responses during cutaneous wound healing in diabetic rats. *Lipids in health and disease*. 10:10.
  12. Li M, Yu H, Pan H, Zhou X, Ruan Q, Kong D, Chu Z, Li H, Huang J, Huang X, Chau A. Nrf2 suppression delays diabetic wound healing through sustained oxidative stress and inflammation. *Front Pharmacol* 10: 1099.
  13. Graziadei PPC, Graziadei GAM. Observations on the ultrastructure of ganglion cells in the circumvallate papilla of rat and mouse. 1978.
  14. Kumar S, Singh R, Vasudeva N, Sharma S. (2012) Acute and chronic animal models for the evaluation of anti-diabetic agents. *Cardiovasc Diabetol*. 11:9.
  15. Yasser, S., & Shon, A. A. (2020). Histomorphometric and Immunohistochemical Study Comparing the Effect of Diabetes Mellitus on the Acini of the Sublingual and Submandibular Salivary Glands of Albino Rats. *Open Access Macedonian Journal of Medical Sciences*, 8(A), 49–54.
  16. Bathina, S., & Das, U. N. (2018). Dysregulation of PI3K-Akt-mTOR pathway in brain of streptozotocin-induced type 2 diabetes mellitus in Wistar rats. *Lipids in health and disease*, 17(1), 168-172.
  17. Hassan, A. M., Abdel-Aziem, S. H., & Abdel-Wahhab, M. A. (2012). Modulation of DNA damage and alteration of gene expression during aflatoxicosis via dietary supplementation of Spirulina (*Arthrospira*) and whey protein concentrate. *Ecotoxicology and environmental safety*, 79(2), 294-300.
  18. Oliva-Hernández R, Fariñas-Medina M, Hernández-Salazar T, Oyarzabal-Vera A, Infante-Bourzac JF, Rodríguez-Salgueiro S, et al. (2022) Repeat-dose and local tolerance toxicity of SARS-CoV-2 FINLAY-FR-02 vaccine candidate in Sprague Dawley rats. *Toxicology*;471:153161.
  19. Slaoui M, Bauchet AL, Fiette L. (2017) Tissue sampling and processing for histopathology evaluation. In: *Methods in Molecular Biology*. Humana Press Inc.101–14.
  20. Ram S, Vizcarra P, Whalen P, Deng S, Painter CL, Jackson-Fisher A, Pirie-Shepherd S, Xia X, Powell EL. (2021) Pixelwise H-score: A novel digital image analysis-based metric to quantify membrane biomarker expression from immunohistochemistry images. *PLoS One*. 16(9):e0245638.
  21. Pai MH, Ko TL, Chou HC. (2007) Effects of streptozotocin-induced diabetes on taste buds in rat vallate papillae. *Acta Histochem*. 109(3):200–7.
  22. Matough, F. A., Budin, S. B., Hamid, Z. A., Alwahaibi, N., & Mohamed, J. (2012). The role of oxidative stress and antioxidants in diabetic complications. *Sultan Qaboos University Medical Journal*, 12(1), 556–569.
  23. Ramani, A., Hazra, T., Mudgil, S., & Mudgil, D. (2024). Emerging potential of whey proteins in prevention of cancer. *Food and Humanity*, 2, 100199.
  24. Kerasiotti, E., Stagos, D., Tzimi, A., & Kouretas, D. (2016). Increase in antioxidant activity by sheep/goat whey protein through nuclear factor-like 2 (Nrf2) is cell type dependent. *Food and Chemical Toxicology*, 97, 47–56.
  25. Kong, F., Kang, S., Zhang, J., Zhao, H., Peng, Y., Yang, M., Zheng, Y., Shao, J., & Yue, X. (2022). Whey protein and xylitol complex alleviate type 2 diabetes in C57BL/6 mice by regulating the intestinal microbiota. *Food Research International*, 157, 111454.

26. Smith, K., Taylor, G. S., Brunsgaard, L. H., Walker, M., Bowden Davies, K. A., Stevenson, E. J., & West, D. J. (2022). Thrice daily consumption of a novel, premeal shot containing a low dose of whey protein increases time in euglycemia during 7 days of free-living in individuals with type 2 diabetes. *BMJ Open Diabetes Research & Care*, 10(3).
27. Mostafa S, Abdou A, Selim KM, Rady R, Rady D. (2023) Investigating the Short-Term Effect of Diabetic Peripheral Neuropathy on Different Neuronal Sub-classes in Circumvallate Papilla in Rats %J Egyptian Dental Journal. 69(4):2771-80.
28. Monteiro MM, D'Epiro TT, Bernardi L, Fossati AC, Dos Santos MF, Lamers ML. (2017) Long-and short-term diabetes mellitus type 1 modify young and elder rat salivary glands morphology. *Archives of Oral Biology*. 73:40-7.
29. Hany K. (2008) Effect of diabetes mellitus on the structure of skeletal muscle in adult male Albino rats and the protective role of chromium: histological and immunohistochemical study. *Egyptian Journal of Histology*. 31 (2): 341-353.
30. Sayed LH, Badr G, Omar HM, Abd El-Rahim AM, Mahmoud MH. (2017) Camel whey protein improves oxidative stress and histopathological alterations in lymphoid organs through Bcl-XL/Bax expression in a streptozotocin-induced type 1 diabetic mouse model. *Biomedicine & pharmacotherapy*. 88:542-52.
31. Hossam Ebaid HE, Al-Tamimi J, Ali Metwalli AM, Ahmed Allam AA, Kairy Zohir KZ, Jamaan Ajarem JA, Ahmed Rady AR, Alhazza IM, Ibrahim KE. (2015) Effect of STZ-induced diabetes on spleen of rats: improvement by camel whey proteins. *Pakistan J. Zool.*, 47(4), pp. 1109-1116.
32. Falkowski M, Maciejczyk M, Koprowicz T, Mikołuc B, Milewska A, Zalewska A, Car H. (2018) Whey protein concentrate WPC-80 improves antioxidant defense systems in the salivary glands of 14-month wistar rats. *Nutrients*.10(6):782.
33. Ngo, V., & Duennwald, M. L. (2022). Nrf2 and Oxidative Stress: A General Overview of Mechanisms and Implications in Human Disease. *Antioxidants*, 11(12), 2345.
34. Drożdżik, A., Wajda, A., Łapczuk, J., & Laszczyńska, M. (2014). Expression and functional regulation of the nuclear receptors AHR, PXR, and CAR, and the transcription factor Nrf2 in rat parotid gland. *European Journal of Oral Sciences*, 122(4), 259–264.
35. Ungvari, Z., Bailey-Downs, L., Gautam, T., Jimenez, R., Losonczy, G., Zhang, C., Ballabh, P., Recchia, F. A., Wilkerson, D. C., Sonntag, W. E., Pearson, K., de Cabo, R., & Csiszar, A. (2011). Adaptive induction of NF-E2-related factor-2-driven antioxidant genes in endothelial cells in response to hyperglycemia. *American Journal of Physiology - Heart and Circulatory Physiology*, 300(4), H1133.
36. Jiang, T., Huang, Z., Lin, Y., Zhang, Z., Fang, D., & Zhang, D. D. (2010). The protective role of Nrf2 in streptozotocin-induced diabetic nephropathy. *Diabetes*, 59(4), 850–860.
37. Kumar A, Mittal R. (2017). Nrf2: a potential therapeutic target for diabetic neuropathy. *Inflammopharmacology*, 25(4):393-402.
38. Dinkova-Kostova, A. T., & Abramov, A. Y. (2015). The emerging role of Nrf2 in mitochondrial function. *Free Radical Biology and Medicine*, 88(Part B), 179–188.
39. To, K., Okada, K., Watahiki, T., Suzuki, H., Tsuchiya, K., Tokushige, K., Yamamoto, M., Ariizumi, S. ichi, & Shoda, J. (2023). Immunohistochemical expression of NRF2 is correlated with the magnitude of inflammation and fibrosis in chronic liver disease. *Cancer Medicine*, 12(19), 19423.
40. Cheng, S. H., Tseng, Y. M., Wu, S. H., Tsai, S. M., & Tsai, L. Y. (2017b). Whey Protein Concentrate Renders MDA-MB-231 Cells Sensitive to Rapamycin by Altering Cellular Redox State and Activating GSK3β/mTOR Signaling. *Scientific Reports*, 7(1).
41. Cheng, S. H., Tseng, Y. M., Wu, S. H., Tsai, S. M., & Tsai, L. Y. (2017a). Selective effects of whey protein concentrate on glutathione levels and apoptosis in rats with mammary tumors. *Food and Chemical Toxicology*, 107, 440–448.